Digest Journal of Nanomaterials and Biostructures Vol. 19, No. 4, October-December 2024, p. 1577-1590

Study on the water and mold resistance of ZnO/polyurethane superhydrophobic coating on circuit boards

J. J. Wang [a], Z. L. Li [a], C. Q. Li [a,*], X. Shen [a], F. H Liang [a], A. Alidad [b]
[a] *School of Materials and Engineering, Jiangsu University of Technology, Changzhou, Jiangsu, 213001*
[a] *Department of Mechanical Engineering, York University, Toronto, ON, M3J 1P3, Canada*

In this work, superhydrophobic coatings were prepared on circuit boards based on the susceptibility of circuit boards to harsh environments such as humidity and mold adhesion, leading to reduced service life. Firstly, cetyltrimethoxysilane and γ-aminopropyltriethoxysilane were used to modify zinc oxide nanoparticles with different particle sizes. Then polyurethane and modified nanoparticles were successively sprayed on the circuit boards with a spraying process, and the superhydrophobic coatings were finally produced. The impact of the zinc oxide mass ratio with different particle sizes, silane coupling agent content, and surface modifier content on the hydrophobicity of the coatings were investigated. The results show that when the mass ratio of zinc oxide (30nm) to zinc oxide (90nm) is 1:1, the silane coupling agent content is 12‰. The surface modifier content is 12‰, the hydrophobicity of the coating is the best, and its CA can be up to 169.5°, and its SA can be up to 2.8°. It exhibits good protection of circuit boards in the tests of adhesion, acid, and alkali corrosion resistance, self-cleaning performance, and anti-mold performance. Performance, so that the coating is in the future field of electronic equipment applications.

(Received July 25, 2024; Accepted October 21, 2024)

Keywords: Superhydrophobic coating, Waterproofing, Mould resistance, Spraying method

1. Introduction

Electronic devices face erosion by water, dust, salt water, and mold during use. For example, water can intrude into the circuit board, eroding the circuit board's electrodes and destroying the electronic equipment [1-4]. Bacteria can multiply rapidly under the right conditions, which induces various diseases and leads to equipment failure [5]. Nowadays, the waterproofing methods of electronic devices include the overall structure, canned adhesive sealing, etc. Still, there are specific problems, such as the overall structure of the parts not being quickly replaced, canned adhesive poor heat dissipation, in the use of the process of severe impact on the service life of the electronic products, which ultimately leads to increase the cost but can not solve the fundamental problem [6].

* Corresponding author: cql6660607@163.com
https://doi.org/10.15251/DJNB.2024.194.1577

To further protect electronic devices from water, dust, and mold, superhydrophobic technology is widely valued for its waterproofing [7, 8], self-cleaning [9-11], and corrosion protection [12,13]. Superhydrophobic surfaces are surfaces where the water contact angle (CA) is> 150° and the sliding angle (SA) is < 10° [14]. At this point, water droplets do not easily intrude into the material's interior. Therefore, by taking advantage of natural phenomena such as cicada wings, dragonfly wings, and lotus leaf surfaces that can effectively hydrophobise, prevent bacteria from adhering, or kill certain types of bacteria [15], scholars have developed superhydrophobic surfaces for electronic devices with these functions. Artificially constructed superhydrophobic surfaces need a certain degree of roughness and low surface energy on the coating surface [16]. Based on the above factors, various methods to prepare superhydrophobic surfaces, such as spraying [17-18], sol-gel [19-20], surface etching [21-22], electrostatic spinning [23-24], and self-assembly [25] have been discovered and widely used. Among these, spraying has been widely used due to its simplicity of operation, minor limitations, wide range of substrates, low cost, and ease of achieving mass production. From the material point of view, ZnO is non-toxic and inexpensive, with high stability and durability. Introducing ZnO NPs in coatings can confer and improve their antimicrobial properties. Therefore, using ZnO NPs as the primary antimicrobial material for coatings is undoubtedly wise. For example, Li [26] et al. prepared superhydrophobic coatings by spraying polymers prepared by blending epoxy resin (EP), polydimethylsiloxane (PDMS), filled with modified SiO_2 on different substrates, which played a significant role in enhancing the coating properties and significantly improved the hydrophobicity of the coatings. Kesavan [27] et al. prepared superhydrophobic perfluoroalkanes (PFAs) on stainless steel surfaces using a cold spraying technique—Fluoroalkane (PFA) coatings with CA of 160° and SA of 6°. Zhang [28] et al. constructed superhydrophobic surfaces on plastic plates by spraying them twice, the first time with micron particles and the second time with nanoparticles and micro- and nano-rough structures were made by spraying them twice, thus constructing superhydrophobic surfaces. However, their performance in preventing the adhesion of bacteria and microorganisms needs to be studied in depth. Biomimetic superhydrophobic coatings have emerged as an effective antimicrobial method [5].

To solve the problem effectively, this paper hydrophobically modifies zinc oxide with different particle sizes and successively sprays polyurethane and modified nanoparticles on the circuit board. The change in wettability, adhesion, durability (PH=1-14, 3.5wt%NaCl), friction resistance, and mildew resistance were among the characteristics of the superhydrophobic coating that were researched. The influence of zinc oxide mass ratio with varying particle sizes, silane coupling agent, and surface modifier content on the hydrophobicity of the coating was also examined.

2. Experimental component

2.1. Experimental materials

Shenzhen Kobi Micro Semiconductor Co. provided the circuit board (green oil single-sided 3 cm x 5 cm), while Guangzhou Changyu Chemical Technology Co. offered the ZnO (30 nm, 90 nm). The supplier of anhydrous ethanol (AR) was Jiangsu Qiangsheng Functional Chemical Co. We bought γ-aminopropyltriethoxysilane (KH550, AR) from Yusuo Chemical Technology Co. in Shandong. Guangdong Wengjiang Chemical Reagent Co. was the supplier of cetyltrimethoxysilane (HDTMS, 85% by mass). The supplier of water-based polyurethane (PU) was Shenzhen Jitian

Chemical Co. Analytically pure sodium hydroxide (NaOH), sodium chloride (NaCl), and hydrochloric acid (HCl) were acquired from Sinopharm Chemical Reagent Co.

2.2. Preparation of superhydrophobic nanocomposite coatings

2.2.1. ZnO hydrophobic modification

ZnO of various particle sizes was added to a solvent combination of anhydrous ethanol and deionized water (based on prior work), and a suitable amount of KH550 was added and agitated at 600 r/min for 1 hour. Following that, a particular amount of HDTMS was added and stirred at 600 r/min for 5 hours to produce the modified solution.

2.2.2. Preparation of superhydrophobic nanocomposite coatings

Pre-treatment of circuit boards: rinse them repeatedly with anhydrous ethanol and deionized water and dry them in an oven. The PU and modified ZnO solution were successively sprayed onto the surface of the pre-treated circuit board using the spraying method. Adjust the distance between the spray gun muzzle and the circuit board to 15 cm at a 2-3 bar relative pressure. Hold the spray gun to move the Z-shaped path, slowly spray on the circuit board, and then dry at room temperature for 24 h,as shown in Fig. 1.

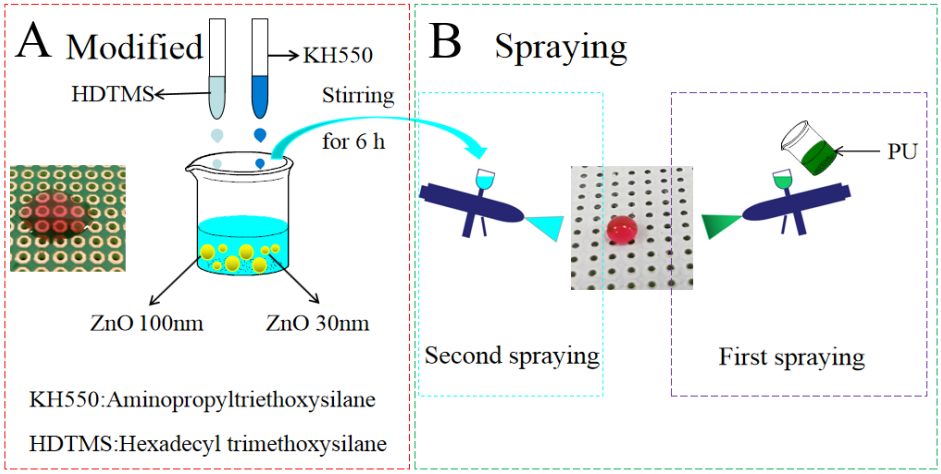

Fig. 1. Preparation process of superhydrophobic coating.

2.3. Structural and wetting characterisation

The chemical composition changes were analyzed using a Fourier transform infrared spectrometer (FTIR, Nicolet iS5, Thermo Fisher Scientific, USA). A thermal field emission scanning electron microscope (SEM, Sigma500, ZESS, Germany) was used to analyze the micro-morphology of the superhydrophobic composite coatings. We utilized an energy spectrometer (EDS, OXFORD) to examine the surface element distribution. Using a water droplet volume of 10 μL, the wettability of the samples was evaluated using a contact angle meter (Krüss, DSA 30). The test was performed five times on the samples, and the average result was used as the test value.

2.4. Performance testing

Adopt the standard for the ASTMD3359 scribing method for the adhesion test of the coating applied to the circuit board; the standard is 5B-0B level for good to bad. Test method: the sample is placed on enough table, with a razor blade force cut through the coating to the bottom layer, with a distance of 2 mm between the six parallel lines, and then the vertical direction of the same six parallel lines, the length of the scratch is 3-4 cm. cleaned up with a soft brush, affixed to the tape, press to ensure that the fit is better, and quickly pulled apart, and the standard grading table compared to the grading, the standard grading table of the adhesion is shown in Table 1 [29].

Table 1. Adhesion standard grading scale.

rank	appearances
5B	The edges of the incision are entirely smooth with no flaking.
4B	Trace flaking at incision junction with ≤5% breakage area.
3B	There is a small amount of flaking at the edge of the incision or the junction, with 5-15% of the area broken. □
2B	Peeling at the edge of the cut or extensive or complete peeling of some grids, with 15-35% of the area damaged
1B	Partial peeling of the cut edges or large or total peeling of part of the lattice, with 35-65% of the area damaged
0B	Patchy peeling at the edge of the incision or the junction, with more than 65% of the area broken off

Corrosion resistance: The samples were submerged in either a pH=1-12 aqueous solution or a NaCl (3.5wt.%) aqueous solution and were removed regularly to be dried and rinsed with deionized water. Following this, the wettability characteristics of the samples were assessed and noted [30].

Friction resistance: Place the sample (15cm^2) under the abrasion test head of the steel wool abrasion tester and tighten it with a fixture, put 50 g test weights on it, set the speed to 40/min, and record the wetting property of the sample surface every 10 times [31].

Anti-mould: The untreated circuit boards and superhydrophobic coating-treated circuit boards are placed on the culture medium and inoculated with spore suspensions using the spraying method, maintaining the culture conditions of temperature (29±1)℃ and relative humidity of 80%, and after 2 days of cultivation, the growth of different molds can be observed with the naked eye on each control strip, or it is ineffective, and it is necessary to start from scratch, and the samples are observed to grow molds after 7 days.

Self-cleaning: Drops of water are placed on the surface of an untreated board covered with cement powder and a board treated with superhydrophobic coating, and the rolling path of the droplets is observed.

3. Results and discussion

3.1. Factors affecting coating wettability

3.1.1. Effect of the preparation process

The rough structure of the material surface affects the wettability of the coating. Using different ZnO particle sizes to create a micro- and nanoscale rough structure, as seen in Fig. 2(A), the effect of the mass ratio of ZnO with varied particle sizes on the hydrophobicity of the coating was examined in this work. At that time, the content of KH550 was 6‰, and the content of HDTMS was 6‰. As can be seen from Fig. 2(A), mixed particle size nanoparticles are more hydrophobic than single particle size nanoparticles, with the contact angle of the coatings constructed with mixed particle sizes mostly above 160° and the rolling angle mostly below 10°. In contrast, the contact angle of the coatings constructed with single particle sizes are all lower than 160°, and the rolling angle is above 10°. This is because the rough structures constructed by nanoscale particles with different particle sizes are more suitable for creating superhydrophobic surfaces than those constructed by nanoparticles with a single particle size. In particular, when using a mass ratio of 1:1 between 90nm ZnO and 30nm ZnO, the coating is more hydrophobic than the coatings constructed with other mass ratios. The contact angle can reach 168° as well, and the rolling angle can reach 3.8°. It demonstrates that the coating performs best in terms of hydrophobicity when the employed mass ratio of ZnO (30 nm) to ZnO (90 nm) is 1:1.

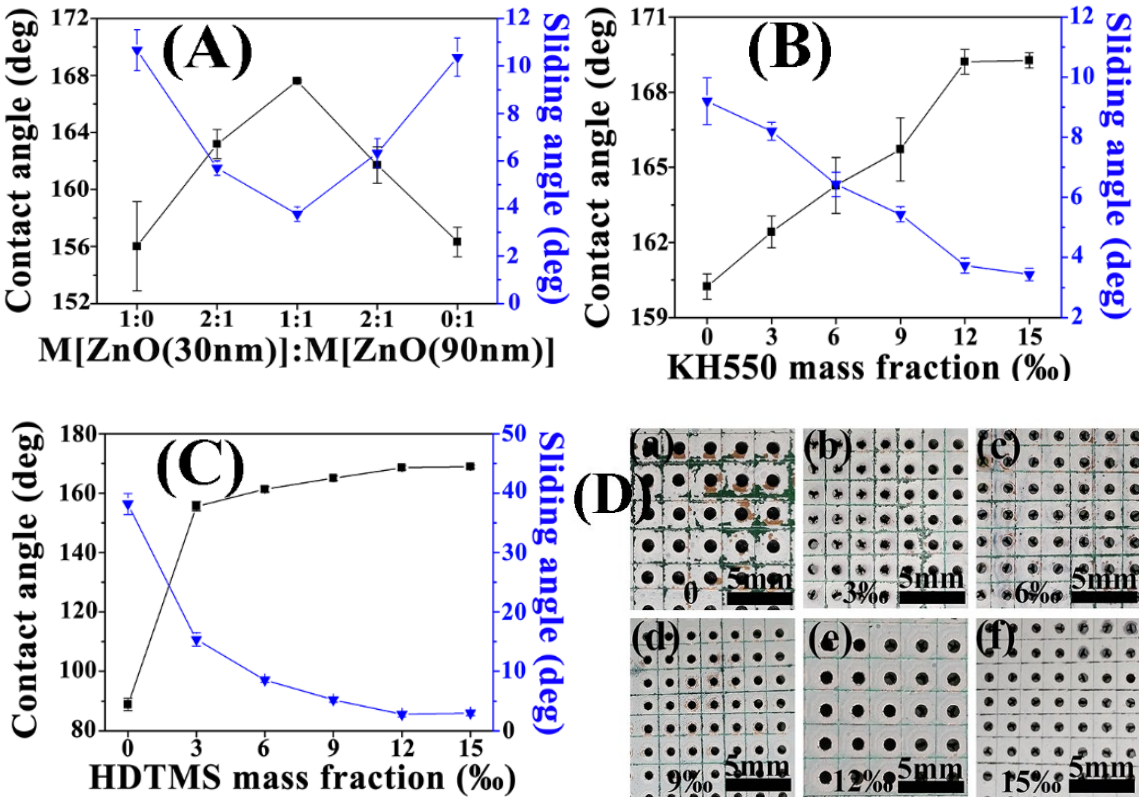

Fig. 2. Effect of the mass ratio of ZnO (30 nm) to ZnO (90 nm) on the hydrophobicity of the coating (A); Effect of the dosage of γ-aminopropyltriethoxysilane on the hydrophobicity of the coating (B); Effect of the dosage of hexadecyltrimethoxysilane on the hydrophobicity of the coating (C); Effect of the dosage of γ-aminopropyltriethoxysilane on the coating Adhesion (D).

Keeping the mass ratio of ZnO (30 nm) to ZnO (90 nm) as 1:1 with the HDTMS content of 6‰ unchanged and other fabrication processes unchanged, the effect of KH550 content on the coating properties was investigated, as shown in Fig. 2(B). Gradually increasing the amount of KH550 used, the hydrophobicity of the coating follows, the contact angle rises, and the rolling angle falls. This is because one end of KH550 consists of three methoxyl groups (-OCH_2CH_3), and after hydrolysis of ethoxyl groups, it condenses and reacts with the hydroxyl groups (-OH) on the surface of ZnO to form silicon-oxygen-silicon-bonds (-Zn-O-Si-), which reduces the surface energy of ZnO, thus decreasing the surface energy of the coatings, and improves the hydrophobicity of the coatings. In the KH550 use concentration up to 12‰, the contact angle of the coating from the unused 159.3° to 169.3°, the rolling angle for the reduction from 11° to 3.8°, after the use of the amount of further increase in the hydrophobicity of the coating increase is not apparent. From the graph in Fig. 2(D), it was found that the adhesion grade of the coating was strengthened from 1B when KH550 was not used to 5B when the amount of KH550 was increased from 12‰ to 15‰, which significantly improved the adhesion of the coating. This is because the -H_2N group carried at one end of KH550 can combine with the -NCO group of PU to form a urea group [32], which increases the adhesion of ZnO to the substrate PU. In summary, the amount of KH550 used was selected to be 12‰, and the coating had the best hydrophobicity and better adhesion.

Keeping the mass ratio of ZnO (30 nm) to ZnO (90 nm) at 1:1, the content of KH550 at 12‰ unchanged, and other fabrication processes unchanged, the effect of the amount of HDTMS used on the hydrophobic properties of the coatings was investigated, as shown in Fig. 2(C). Low surface energy is a critical factor in constructing superhydrophobic surfaces. Additionally, HDTMS decreases the coating's surface energy, enhancing the hydrophobicity of the layer. When no HDTMS is added, the contact angle is 90°, and the rolling angle is 40.3°, indicating that the coating does not exceed hydrophobicity standards. However, when the content of HDTMS is high, the coating's surface energy decreases, and its hydrophobicity increases. When HDTMS content is 12‰, the contact angle is the largest at 169.5°, and the rolling angle is the smallest at 2.8°. As the content of HDTMS increases, the contact angle and rolling angle remain stable due to the low surface energy, which is difficult to reduce further. In summary, the HDTMS content is selected at 12‰.

3.1.2. Influence of surface chemical composition and morphology

Spectrum lines a, b, and c are contrasted with spectral line d in the A plot, as seen in Fig. 3. The telescopic vibrational peaks of -CH_3 and -CH_2 formed by HDTMS on the ZnO surface are 2917.54 cm^{-1} and 2849.66 cm^{-1}. The C-O bonding stretching vibrational peaks are 1466.72 $cm^{-1,}$ and the vibrational peak generated by the -COOR of HDTMS is 1406.93 cm^{-1}.

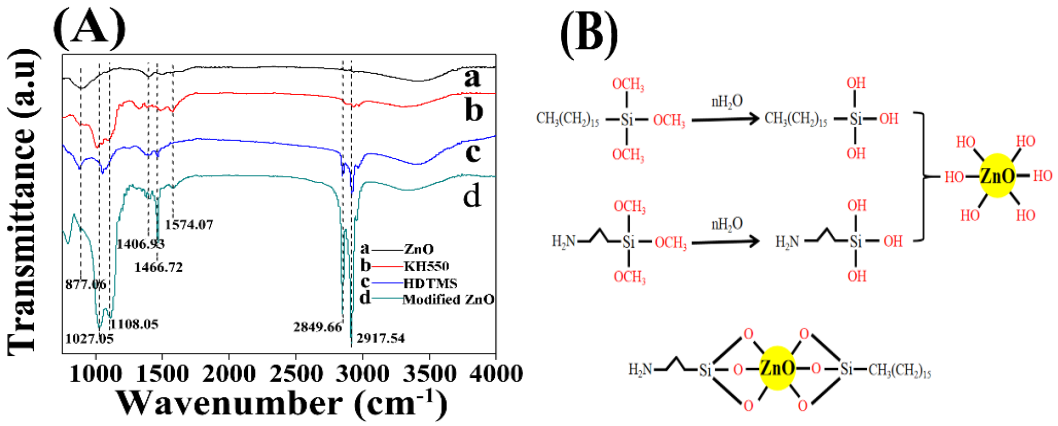

Fig. 3. IR spectra of different samples (A); possible reaction mechanism of ZnO modification by KH550 and HDTMS (B).

The anti-symmetric bending vibrational absorption of -CH_3 and -CH_2 is responsible for 1574.07 cm^{-1}. When HDTMS and KH550 react with ZnO to produce the Si-O-Si bond, two vibrational peaks are formed: antisymmetric contraction at 1108.05 cm^{-1} and symmetric contraction at 1027.05 cm^{-1} [33]. The contraction vibrational peak of the Zn-O bond is 877.06 cm^{-1}. It is created by the dehydration reaction with -OH on the ZnO surface following the hydrolysis of KH550 and HDTMS to Si-OH [34]. The reaction mechanism of HDTMS and KH550 with ZnO is shown in Fig. 3(B), in which KH550 and HDTMS react with water to Si-OH and then hydrolyze and condense with the -OH on the surface of ZnO to achieve the modification of ZnO. The -H_2N group at the other end of KH550 can be combined with the -NCO group of the polyurethane to form the urea group, which increases the adhesion of ZnO to the base polyurethane. The role of HDTMS is that after the hydrolysis of ZnO, the formation of -$CH_3(CH_2)_{15}$ at the other end promotes the lowering of the surface energy of ZnO, thus achieving the effect of superhydrophobicity.

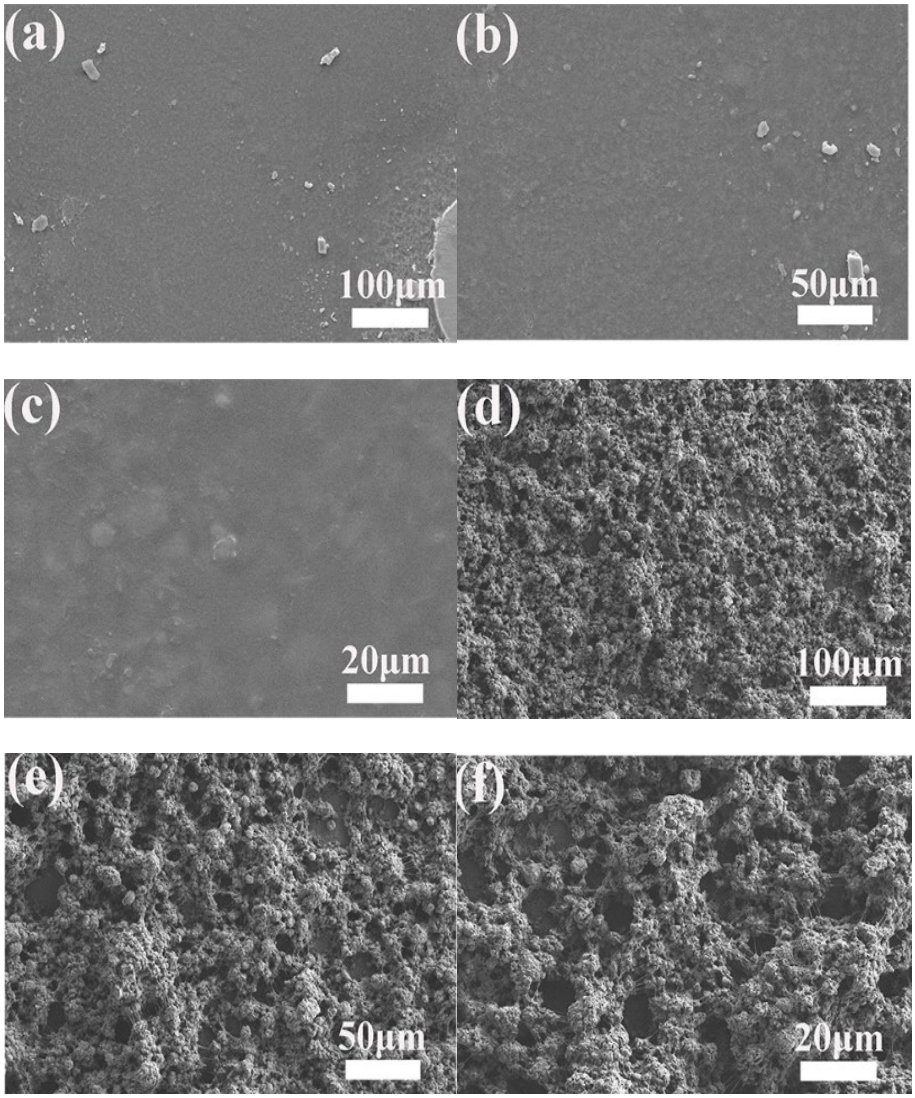

Fig. 4. SEM of untreated board surface (a-c); SEM of superhydrophobic coating treated board surface (d-f).

Table 2. EDS comparison between untreated and superhydrophobic coating treated circuit boards.

Element Element At% PCB	Unprocessed boards	Superhydrophobic coating of circuit boards
C	77.49	55.9
N	03.78	0.3
O	10.81	31.3
Si	00.73	02.2
Zn	00.04	10.4

To better investigate the hydrophobic mechanism of the coated surface, SEM tests were carried out on the untreated circuit boards, and the superhydrophobic coated treated circuit boards and the surface SEM are shown in Fig. 4. The untreated circuit boards' surface morphology is seen in Fig. 4(a-c). The a-plot shows that the untreated circuit boards' surface contains irregular, loosely organized rough features. However, the c-plot's glossy surface lacks any noticeable rough structures, suggesting that the untreated circuit boards' surface rough structures are insufficient to supply the rough structures needed to build the superhydrophobic surfaces. Fig. 4(d-f) shows the surface morphology of the superhydrophobic coated circuit boards. From the d-plot, it is evident that there are condensed nanoparticles on the surface of the coating, and these particles are formed by the stacking of ZnO nanoparticles with different particle sizes sprayed on the urethane, which constructs the rough structure required for superhydrophobicity. They are increasing the adhesion of the nanoparticles to the board, giving the coating both better superhydrophobicity and stability. To further illustrate the composition of the coating, the untreated circuit boards and the superhydrophobic coating treated circuit boards were analyzed by energy spectrum, as shown in Table 2, from which it can be found that the Zn element of the superhydrophobic coating treated circuit boards is significantly increased, which is due to the addition of ZnO particles in the coating, which leads to an increase in the element of Zn, and the increase in the component of Si, which is due to the use of KH550, HDTMS. It can be found that the adhesion of ZnO to polyurethane was successful, and the grafting of KH550 and HDTMS on ZnO was successful.

3.2. Stability analysis

3.2.1. Corrosion resistance

In daily life, harsh environments can severely impact electronic device use, and some erosion problems such as acid rain and seawater will be encountered, so the preparation of circuit boards with solid corrosion resistance is an urgent need for people nowadays. The samples were submerged in NaCl (3.5wt%) or aqueous solutions with varying pH values. The samples were removed on a regular basis to be cleaned and allowed to dry, after which the variations in the sample surface's wettability were noted. Fig. 5(A) illustrates the wettability relationship following the samples' 12-hour immersion in various pH solutions. The wettability relationship of the samples submerged in a NaCl (3.5wt%) solution over time is displayed in Fig. 5(B).

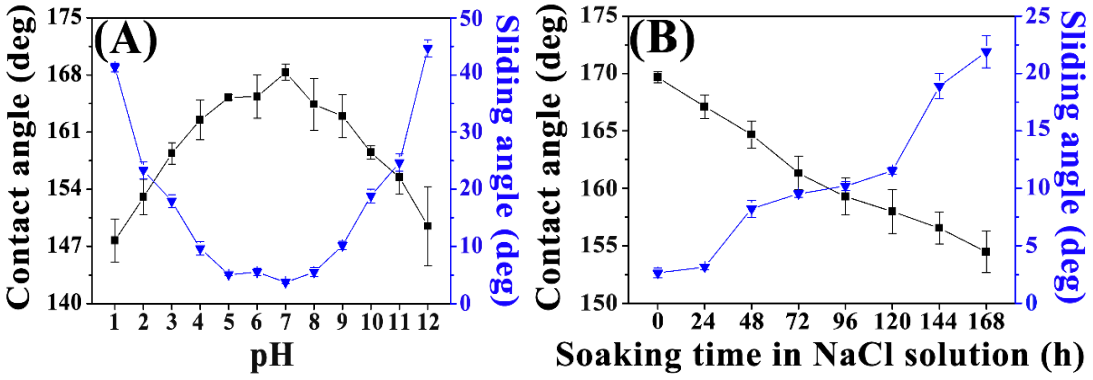

Fig. 5. Wettability relationships of samples immersed in different pH solutions for 12 h (A); wettability relationships of samples immersed in NaCl (3.5wt%) solution for various times (B).

Fig. 5(A) shows that when acid and alkali are strengthened, the contact angle declines, and the rolling angle rises. Specifically, the contact angle declines by approximately 20°, and the rolling angle rises by approximately 40° in floating. However, even after being submerged for 12 hours in a solution of pH=1 and pH=12, the contact angle remains between 154° and 153°, which still exacerbates the need for superhydrophobicity. It also satisfies the standards for superhydrophobic contact angles greater than 150° and rolling angles of fewer than 10° in the pH 5-9 range. This means the samples are more resistant to acids and alkalis, broadening the board's application range.

Fig. 5(B) shows that, following a 48-hour immersion in a 3.5wt%NaCl solution, the rolling angle rose by 6°, and the contact angle dropped by about 5°, both remaining in the superhydrophobic condition. Following 168 hours of submersion, the rolling angle rose by 19°, and the contact angle dropped by around 15°. Because the coating surface's rough structure had been destroyed, the rolling angle was no longer superhydrophobic. While the hydrophobic structure of the coating surface was damaged by Na^+ and Cl^-, which then infiltrated the coating and destroyed the samples, the hydrophobicity of the coatings remained good after 168 hours, indicating the excellent hydrophobicity of the samples in the 3.5wt.%NaCl solution. Overall, the contact angle decreased steadily with the increase in immersion time, and the rolling angle significantly increased after 120 hours, which was caused by the rise in immersion time. The results indicate the outstanding stability performance of the sample in 3.5wt.%NaCl solution.

In conclusion, the low surface energy of the superhydrophobic coated circuit boards and the surface's micro-nano rough structure are responsible for the samples' strong corrosion resistance. The former allows the coating to repel solutions. At the same time, the latter permits air to be stored within the surface's micro-nano roughness, forming an air layer that shields the boards from other corrosive media. These two factors enhance the samples' corrosion resistance and coating stability.

3.2.2. Coating abrasion resistance test

Fig. 6(A) illustrates the correlation between the quantity of rubbings and the materials' wettability, while Fig. 6(B) displays the SEM of samples used 50 times on the steel wool friction resistance tester.

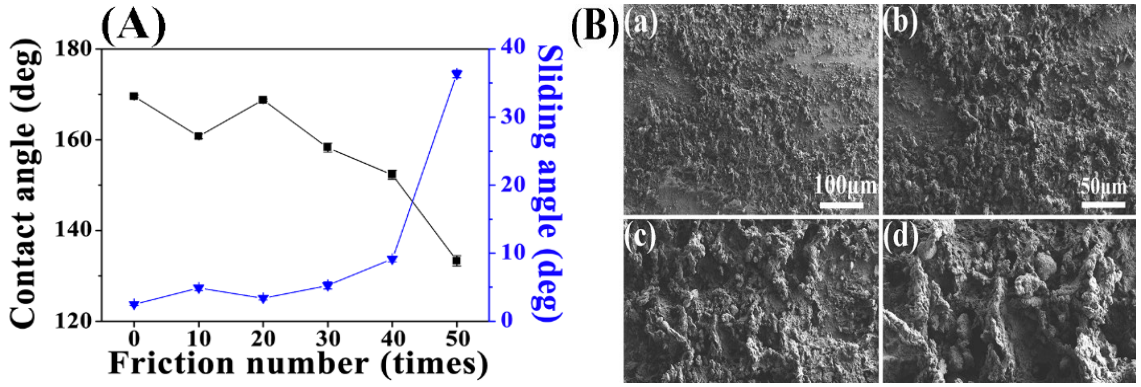

Fig. 6. Plot of the number of rubbing times of the samples versus wettability (A); SEM of the surface of the samples worn 50 times on the steel wool friction tester (B).

As shown in Fig. 6(A), the coating contact angle decreases with the number of abrasions but increases at 20 times due to the abrasion that exposes the nanoparticles buried in the PU, creating a rough structure. The CA was 152.4°, and the SA was 9.8° at 40 times, which is still superhydrophobic. It is evident from (a) of Fig. 6(B) that the coating surface has partially peeled off and from Fig. 6(d) that the coating still has a rough structure. Still, it is no longer noticeable, indicating that the board can only be wettable at the hydrophobic stage. Overall, though, the coating's durability is great [35].

3.3. Anti-mould and self-cleaning properties

The untreated circuit boards and superhydrophobic treated circuit boards against mold are shown in Fig. 7. The untreated circuit board has been covered by mold all around, the surface has also been eroded by mold, and the pores have been filled with mold. Overall the untreated circuit board has been seriously eroded by mold. Superhydrophobic treatment of the circuit board, not covered by mold around, the surface is not eroded by mold, and the pores without the appearance of mold, overall, superhydrophobic treatment of the board's anti-mold performance is remarkable. Super-hydrophobic treatment of the circuit board anti-mould performance is significantly attributable to the coating surface of the ZnO nanoparticles, the chemical mechanism of its anti-mold: when ZnO comes into contact with the mold, ZnO converts to Zn^{2+}, and the combination of organic matter in the mold causes structural and cellular damage, thereby achieving the role of anti-mold. Moreover, the physical mechanism of anti-mold is based on the coating's micro-nanometer rough surface, which allows air to be stored and forms an air layer that helps isolate molds by preventing them from sticking to and submerging in the sample. The processes mentioned above work in concert to provide the samples with anti-mold solid performance.

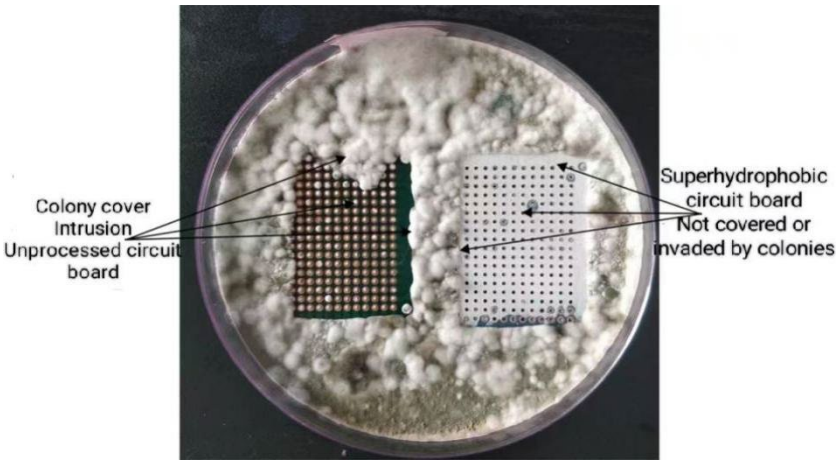

Fig. 7. Mould protection of untreated and superhydrophobic treated circuit boards.

The samples' ability to self-clean when exposed to dust that simulates cement powder is seen in Fig. 8. The samples in the picture were tipped at a 10° angle, and droplets of water were gradually dripped through a dropper located at the upper end of the sample, one centimeter below the surface. It was found that the self-cleaning effect could not be achieved when water droplets were put over an untreated circuit board surface because the droplets fused with the dust and stuck to the surface. Nevertheless, at the same height, the water droplets would remove the dust from the route as they rolled down on the sample surface. This is seen in Fig. 8(b), where it is clear that the water droplets' path is clean and dry, demonstrating a strong self-cleaning effect.

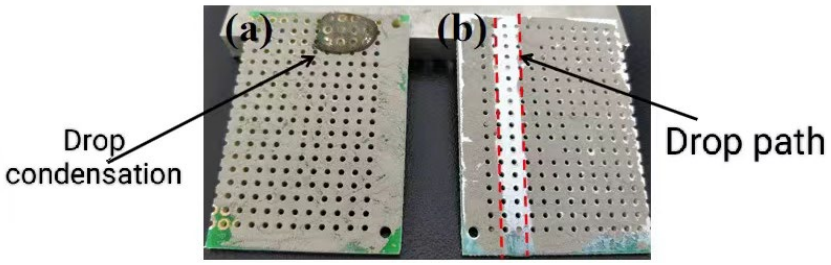

Fig. 8. Self-cleaning behavior of untreated and superhydrophobic coated PCBs: water droplets coalesce on untreated PCB (a); cement dust washes away from superhydrophobic coated PCB surface (b).

4. Conclusion

Electronic devices face water, dust, salt water, and mold erosion. Therefore, a superhydrophobic coating was prepared on the circuit board to improve its durable corrosion resistance. The hydrophobicity of the superhydrophobic surface enhances the circuit boards' water resistance, and the zinc oxide nanoparticles' anti-mold efficacy increases their service life. This paper prepared a zinc oxide/polyurethane composite superhydrophobic coating by combining inexpensive functional nanoparticles with polymers as raw materials. Using an energy spectrometer, scanning

electron microscope, infrared spectrometer, and contact angle measuring device, the samples' wettability, surface morphology, and surface chemical composition were also examined. The properties of the coating, such as acid and alkali resistance, salt solution resistance (3.5wt.%NaCl solution), friction and wear performance, and mildew resistance, etc., were investigated, and the following conclusions were drawn:

(1) a ZnO/polyurethane superhydrophobic coating was created by spraying one step at a time. Using a contact droplet angle meter, its CA was determined to be 169.5° and SA to be 2.8°. Using a scanning electron microscope, it was possible to observe that the surface of the circuit board treated with a superhydrophobic coating exhibited superior hydrophobicity compared to the untreated surface. This difference was primarily due to a modification in the rough structure.

(2) The samples were tested for adhesion level after the sample adhesion level reached 5 B.

(3) The samples showed good corrosion resistance, especially in acid and alkaline solutions in the pH range of 5-9. The samples showed a decrease of 15° in CA and an increase of 19° in SA after 168 h in salt solution (3.5wt.%NaCl solution).

(4) The mold-proof performance of electrical and electronic devices meets grade 0, which has appropriate mold-proof capabilities, following the GB/T 2423.16-2008 environmental test. In terms of its anti-mold and self-cleaning capabilities, it also offers a wide range of application possibilities.

Acknowledgements

This work was supported by the National Natural Science Foundation of China (52073127) and the Changzhou International Cooperation Programme (KYZ23033).

References

[1] S. Zou, X. Li, C. Dong, K. Ding, K. Xiao, Electrochim. Acta. 114(2013)363-371; https://doi.org/10.1016/j.electacta.2013.10.051

[2] X. Wang, Y. Guo, J. Liu, Q. Qiao, J. Liang, J. Environ. Manag. 91(2010)2505-2510; https://doi.org/10.1016/j.jenvman.2010.07.014

[3] S. Wan, Y. Cong, D. Jiang, Z. H. Dong, Colloids Surf. A Physicochem. Eng. Aspects. 538(2018)628-638; https://doi.org/10.1016/j.colsurfa.2017.11.056

[4] A. Skwarek, K. Witek, J. Ratajczak, Microelectron. Reliab. 49(2009)569-572; https://doi.org/10.1016/j.microrel.2009.02.026

[5] Y. Zhan, S. Yu, A. Amirfazli, A. Rahim Siddiqui, W. Li, Adv. Eng. Mater. 24(2022); https://doi.org/10.1002/adem.202101053

[6] S. M. Emarati, M. Mozammel, Ceram. Int. 46(2019)1652-1661; https://doi.org/10.1016/j.ceramint.2019.09.137

[7] W. Wang, K. Lockwood, L. M. Boyd, M. D. Davidson, S. Movafaghi et al., Acs. Appl. Mater. Inter. 8(2016) 18664-18668; https://doi.org/10.1021/acsami.6b06958

[8] R. Mohammadi, J. Wassink, A. Amirfazli, Langmuir. 20(2004)9657-9662;

https://doi.org/10.1021/la049268k

[9] T. Zhu, S. Li, J. Huang, M. Mihailiasa, Y. Lai, Mater. Des. 134(2017)342-351; https://doi.org/10.1016/j.matdes.2017.08.071

[10] H. R. Byun, Y. G. Ha, J. Nanosci Nanotechno. 17(2017)5515-5519; https://doi.org/10.1166/jnn.2017.13805

[11] J. Zhang, C. Zhu, J. Lv, W Zhang, J. Feng, ACS Appl. Mater. Interfaces. 10(2018)40219-40227; https://doi.org/10.1021/acsami.8b12567

[12] T. Xiang, Y. Han, Z. Guo, R. Wang, S. Zheng, S. Li, C. Li, X. Dai, ACS Sustain. Chem. Eng. 6(2018)5589-5606; https://doi.org/10.1021/acssuschemeng.8b00639

[13] Y. Liu, Q. Wu, C. Wang, D. Zhou, R. Liang, Y. Kang, Polym. Test. 70(2018)1-7; https://doi.org/10.1016/j.polymertesting.2018.06.022

[14] H. Li, S. Yu, Appl. Surf. Sci. 420(2017)336-345; https://doi.org/10.1016/j.apsusc.2017.05.131

[15] A. Tripathy, P. Sen, B. Su, W. H. Briscoe, Adv. Colloid Interface Sci. 248(2017)85-104; https://doi.org/10.1016/j.cis.2017.07.030

[16] C. Aulin, S. H. Yun, L. Wågberg, T. Lindström, ACS Appl. Mater. Interfaces. 1(2009)2443-2452; https://doi.org/10.1021/am900394y

[17] X. Kong, C. Zhu, J. Lv et al., Prog. Org. Coat. 138(2020)105342-105342; https://doi.org/10.1016/j.porgcoat.2019.105342

[18] X. Zhang et al., Chem. Eng. J. 1(2019)276-285; https://doi.org/10.1016/j.cej.2019.04.040

[19] X. Wu, Q. Fu, D. Kumar, J. W. C. Ho, P. Kanhere, H. Zhou, Z. Chen, Mater. Des. 89(2016)1302-1309; https://doi.org/10.1016/j.matdes.2015.10.053

[20] Z. Jiang, S. Fang, C. Wang, H. Wang, C. Ji, Appl. Surf. Sci. 390(2016)993-1001; https://doi.org/10.1016/j.apsusc.2016.08.152

[21] W. Ban, S. Kwon, J. Nam, J. Yang, S. Jang, D. Jung, Thin Solid Films. 641(2017)47-52; https://doi.org/10.1016/j.tsf.2017.02.007

[22] P. Tao, W. Shang, C. Song, Q. Shen, F. Zhang, Adv. Mater. 27(2015)428-463; https://doi.org/10.1002/adma.201401449

[23] J. Wu, X. Li, Y. Wu, G. Liao, P. Johnston, P. D. Topham, L. Wang, Appl. Surf. Sci. 422(2017)769-777; https://doi.org/10.1016/j.apsusc.2017.06.076

[24] M. Spasova, N. Manolova, N. Markova, I. Rashkov, Appl. Surf. Sci. 363(2016):363-371; https://doi.org/10.1016/j.apsusc.2015.12.049

[25] J. Mao, M. Ge, J. Huang, Y. Lai, C. Lin, K. Zhang, J. Mater. Chem. A. 5(2017)11873-11881; https://doi.org/10.1039/C7TA01343D

[26] D. Li, L. Ma, B. Zhang, S. Chen, Nanoscale. 367(2019)169-179; https://doi.org/10.1039/D0NR08985K

[27] K. Ravi, W. L. Sulen, C. Bernard, Y. Ichikawa, K. Ogawa, Surf. Coat. Technol. 373(2019)17-24; https://doi.org/10.1016/j.surfcoat.2019.05.078

[28] L. Zhang, X. Xue, H. Zhang, Z. Huang, Z. Zhang, Compos. Part A Appl. Sci. Manuf. 146(2021)106-405; https://doi.org/10.1016/j.compositesa.2021.106405

[29] X. Shen, T. Mao, C. Li, F. Mao, Z. Xue, G. Xu, A. Alidad, Prog. Org. Coat.

181(2023)107602; https://doi.org/10.1016/j.porgcoat.2023.107602

[30] H. Li, S. Tu, H. Tu, M. Chen, S. Zhou, L. Wu, Chem. Eng. J. 483(2024)149319; https://doi.org/10.1016/j.cej.2024.149319

[31] L. Shi, H. Yan, S. Zhao, L. Zhang, X. Fan, Appl. Surf. Sci. 655(2024)159662; https://doi.org/10.1016/j.apsusc.2024.159662

[32] G. Dong Feng, Y. Ma, M. Zhang, P. You Jia, Prog. Org. Coat. 133(2019)267-275; https://doi.org/10.1016/j.porgcoat.2019.04.053

[33] S. Yuan, K. Li, Y. Sun, C. Cong, Y. Liu, D. Lin, L. Pei, Y. Zhu, H. Wang, Chem. Eng. J. 472(2023)144881; https://doi.org/10.1016/j.cej.2023.144881

[34] X. L. Wei, N. Li, W. J. Yi, L. J. Li, Z. S. Chao, Surf. Coat. Technol. 325(2017)565-571; https://doi.org/10.1016/j.surfcoat.2017.06.004

[35] M. Bharathia , K. N. Anuradhaa, M. V. Murugendrappab,Digest Journal of Nanomaterials and Biostructures,Vol.18, No.1, January-March 2023, p.343-365 ; https://doi.org/10.15251/DJNB.2023.181.343